Activity standardization of 60Co and 106Ru/106Rh by means of the TDCR method and the importance of beta spectrum

Christophe Bobin, Cheick Thiam, M.-D. M'Hayham, Xavier Mougeot

Activity standardization of ^{60}Co and ^{106}Ru/^{106}Rh by means of the TDCR method and the importance of the beta spectrum

Bobin, C.[1], Thiam, C.[1], M'Hayham, M.-D.[1], Mougeot, X.[1]

[1]Université Paris-Saclay, CEA, List, Laboratoire National Henri Becquerel (LNE-LNHB), F-91120 Palaiseau, France

Corresponding author: christophe.bobin@cea.fr

Abstract

Atomic and nuclear data represent an important input for the accuracy of primary activity measurements based on liquid scintillation. In particular, the reliability of β-spectrum computation has been investigated for several years through experimental and theoretical studies providing solid evidence for the need to consider the atomic effects. In the present study, the activity standardization of two β-emitting radionuclides (^{60}Co, ^{106}Ru/^{106}Rh) was carried out by means of the 4πβ–γ coincidence and Triple-to-Double Coincidence Ratio (TDCR) methods. The comparison between the activity concentrations given by both primary techniques presents new evidence that a better agreement is obtained when the exchange and screening effects are included in the β-spectra implemented in the model of light emission for TDCR measurements. A new development of a stochastic model based on Geant4 simulations for TDCR calculations is also presented.

Keywords: Activity standardization; liquid scintillation counting, TDCR, 4πβ-γ coincidence counting, β-spectra.

1. Introduction

In the radionuclide metrology field, the TDCR method (Triple to Double Coincidence Ratio) is an important measurement technique based on liquid scintillation (LS) dedicated to primary activity standardization (Broda et al., 2007). Its implementation requires the use of a specific three-photomultipliers (PMTs) detection system allowing the counting of double and triple coincidences from which the TDCR value is measured. This experimental result is used in the detection efficiency calculation by means of a statistical model of light emission that includes the atomic and nuclear data of the radionuclide to be measured. As a consequence, the accuracy of TDCR activity measurements is directly related to the precise knowledge of this important modelling input. In that context, several studies based on β-spectrometry using cryogenic detectors led to evidence that theoretical calculations can be improved by including the atomic effects (Gaitskell et al., 1996; Angrave et al., 1998; Mougeot et al., 2012; Loidl et al., 2014). Indeed, the screening and exchange effects in β-decay (Mougeot and Bisch, 2014) can significantly increase probabilities of β-emission at low energies (lower than 20 keV) which can, if unaccounted, yield systematic deviations in LS primary measurements. This issue was also investigated by comparing the CIEMAT/NIST efficiency tracing and TDCR methods (Broda et al., 2007) for various radionuclides such as ^{63}Ni (Kossert and Mougeot, 2015), ^{60}Co (Kossert et al., 2018) and ^{90}Sr/^{90}Y (Kossert and Mougeot, 2021). The findings of these studies have shown an improvement of the accuracy of LS activity measurements when the atomic effects are taken into account.

As described by Kossert et al. (2018) for ^{60}Co activity measurements, the problem of β-spectra calculations can also be investigated by comparing TDCR and 4πβ–γ coincidence counting in the case of β–γ emitting radionuclides. The 4πβ–γ coincidence method presents the advantage of assessing activity independently from the calculation of β-spectra (Campion, 1959;

Bobin, 2007). In the framework of the participation of LNE-LNHB to the pilot study CCRI(II)-P1.Co-60 in 2021, this paper presents a new comparison of activity measurements of ^{60}Co between the TDCR and 4πβ–γ coincidence methods. Cobalt-60 ($T_{1/2}$ = 5.2711 (8) a) disintegrates by β^- emission to excited levels of ^{60}Ni (Bé et al., 2006) followed by two coincident γ-transitions (1173 keV and 1332 keV). In this case, the 4πβ–γ coincidence method was implemented using a proportional counter (PC) in the β-channel in order to reach the best accuracy on activity measurements. A comparison is also presented in the case of activity measurements of ^{106}Ru/^{106}Rh. Ruthenium-106 disintegrates through β^- emission with maximum β-energies of 39.4 keV ($T_{1/2}$(^{106}Ru) = 371.5 (21) d). The daughter radionuclide ^{106}Rh also disintegrates by β^- emission with maximum β-energies ranging from 144 keV to 3.55 MeV ($T_{1/2}$(^{106}Rh) = 30.1 (3) s) to the ground state (78.80 (24)%) and to 36 excited levels of ^{106}Pd (Bé et al., 2016). The main γ-photon emissions are: ~ 512 keV (~ 20.5%), ~ 622 keV (~ 9.9%) and ~ 1050 keV (~ 1.5%). The 4πβ–γ coincidence method was carried out by means of a liquid scintillation (LS) detection system equipped with a three-PMTs TDCR set-up in the β-channel and by setting a detection threshold to avoid counting from ^{106}Ru decay emission similarly to the activity standardization of ^{68}Ge/^{68}Ga (da Silva et al., 2017; Bobin et al., 2018). The study of the influence of β-spectrum calculation on TDCR measurements is focused on ^{106}Ru. The analysis of TDCR measurements for ^{60}Co and ^{106}Ru/^{106}Rh was based on a stochastic model (Kossert and Grau Carles, 2010) using energies released in the LS cocktail calculated with the Monte Carlo code Geant4 (Agostinelli et al., 2003).

2. Main aspects of theoretical calculations of beta spectra using the BetaShape code

The β-spectra were calculated using the BetaShape code developed at LNHB with and without taking into account the atomic effects. The vast majority of the transitions are of allowed or forbidden unique nature and can be computed with good accuracy. A few number

of transitions in ^{106}Rh decay are of unknown nature due to missing information on the spins and parities of ^{106}Pd excited states, and were treated as allowed. Two other transitions of very low intensities are first forbidden non-unique, requiring nuclear structure information, and were treated as allowed according to the ξ-approximation (Mougeot, 2015).

A summary of the main ingredients of the theoretical modelling can be found in a recent review of the log *ft* values (Turkat et al., 2023). Compared to the version 2.2 of the BetaShape code, the most important improvements relevant to the present study concern the atomic screening and exchange effects. The analytical approach from Bühring (1984) to correct for the former was replaced by an extensive tabulation of relevant screened-to-unscreened parameters determined from full numerical solving of the Dirac equation, which was detailed in Mougeot and Bisch (2014).

The formalism of the exchange effect, which comes from the indistinguishability of the electrons, was originally developed for the allowed transitions by Pyper and Harston (1988). In our first study (Mougeot and Bisch, 2014), only the contribution of the $s_{1/2}$ atomic orbital was considered. Later on, the $p_{1/2}$ orbitals were also taken into account (see e.g. (Aprile, 2020)) and we recently extended the formalism to the forbidden unique transitions (to be published). With regard to the present study, the correction of the exchange effect on the allowed transitions vastly dominates, its contribution to forbidden transitions being negligible due to their weak intensities.

3. Experimental instrumentations

For the present study, the 4πβ–γ coincidence method was implemented by means of a live-timed anticoincidence system inspired from the instrumentation described by Baerg et al. (1976). For that purpose, the anticoincidence technique is performed using specific home-made electronic modules developed at LNHB. Two MTR2 modules (Bouchard, 2000) designed to implement the live-time technique combined to extending dead-times are operated for the

counting in both β- and γ-channels. Regarding the β-channel, the MTR2 module is connected either to a pill-box proportional counter filled with CH_4 gas at atmospheric pressure in the case of 4π(PC)β–γ coincidence counting or to a complete three-PMTs (XP2020Q) set-up designed for TDCR and 4π(LS)β–γ coincidence measurements. LS counting in the β-channel is triggered by double coincidences between PMTs. The γ-channel is equipped with a classical 3"×3" NaI(Tl) scintillator detector. The γ-counting and the associated dead-time is managed with a MTR2 module using the busy pulses delivered by an analog-to-digital converter (Lecroy ADC 3512 module) fed with signals provided by a shaping amplifier. The design of the MTR2 module makes it possible to include the discrimination time of γ-pulses in the extending dead-time implementation.

Basically, the anticoincidence technique refers to indirect measurements of coincidences without the use of a resolving time. To this end, a common channel is implemented by means of a logical ‘‘OR’’ combination between the extending dead-times generated in both the β- and γ-channels. A delay longer than the time-jitter between both β- and γ-events is also imposed in the γ-channel. As a result, the counting in the common channel is triggered by β- and non-correlated γ-pulses. The coincidence rate is then obtained by subtracting the non-correlated γ-rate from the whole γ-rate (both previously corrected for background and live time). At LNHB, this operation is performed by recording two γ-spectra (whole and non-correlated) both corrected for their respective live times. The non-correlated γ-spectra and the associated live time are obtained using the MI1 and MI2 home-made modules (Bouchard, 2002) which are connected to the Lecroy ADC 3512 module and its associated histogram memory module (Lecroy 3588) for the classification of non-correlated γ-events. The acquisition of whole and non-correlated γ-spectra enables off-line analysis of coincidence counting using different γ-windows from a single measurement.

TDCR measurements were carried out using two different instrumentations. In the case of ^{60}Co measurements, the RCTD1 apparatus equipped with three BURLE 8850 PMTs was applied associated to a MAC3 module (Bouchard and Cassette, 2000) operating with a resolving time equal to 40 ns and a minimum extending dead-time set to 50 μs. Regarding ^{106}Ru/^{106}Rh measurements, the detection system equipped with a three-PMTs (XP2020Q) set-up was the same as used in the β-channel of the 4π(LS)β–γ coincidence setup. In that case, a modified MAC3 module was applied enabling a longer resolving time equal to 100 ns. A minimum extending dead-time was also set to 50 μs.

4. Activity measurements of ^{60}Co

4.1 Source preparation

For the participation to the CCRI(II)-P1.Co-60 pilot study, the stock solution of $CoCl_2$•$6H_2O$ had a Co carrier concentration equal to 45 μg/g in 0.1 mol/L of HCl solution. The activity concentration was approximately equal to 100 kBq/g at the reference date. For 4π(PC)β–γ coincidence measurements, nine solid sources were prepared by depositing weighed aliquots of the stock solution on gold-coated VYNS films using the pycnometer method (Sibbens and Alzitzoglou, 2007) and subsequently dried in a ventilated cupboard operating with heated air at 60°C (masses ranging from 9 mg to 25 mg). For TDCR measurements, six LS sources were prepared in standard (low potassium) 20 mL glass vials filled with 10 mL of Ultima Gold (UG) cocktail plus weighed aliquots of the stock solution (masses ranging from 42 mg to 58 mg). Six LS sources were also prepared with standard 20 mL glass vials filled with 10 mL of Hionic Fluor (HF) cocktail (masses ranging from 50 mg to 56 mg).

4.2 4π(PC)β–γ anticoincidence measurements

The activity concentration assessed by means of 4π(PC)β–γ anticoincidence measurements was obtained using the solid sources. The efficiency extrapolation technique was implemented by adding gold-coated foils (Baerg, 1973). In the present study, these measurements were carried out to verify the experimental value of the extrapolation slope obtained from previous measurements with the same detection system. For each 4πβ–γ measurement, coincidence counting was determined using a γ-window centered on the two main γ-energies (1173 keV and 1332 keV). With this setting, the ratio $\frac{N_c}{N_\gamma}$ ranged between 0.86 and 0.953 (N_c and N_γ correspond to the coincidence- and γ-counting rates respectively). The fit of thirteen 4πβ–γ measurements was implemented using the classical straight line equation depending on the variable $\frac{\left(1-{N_c}/{N_\gamma}\right)}{{N_c}/{N_\gamma}}$. The y-intercept yielded an activity concentration equal to 100.58 (14) kBq/g at the reference date. The maximum correction due to the extrapolation technique was about 0.1%. The uncertainty budget is displayed in Table 1.

4.3 TDCR measurements and analysis

The two batches of LS sources prepared with UG and HF cocktails respectively were measured using the RCTD1 detection system. The counting rate of double coincidence counting was about 5000 s^{-1} and the maximum experimental TDCR values were approximately equal to 0.969 for UG sources and 0.958 for HF sources. For activity determination, the analysis of the experimental data was performed according to a stochastic approach described by Kossert and Grau Carles (2010) and based on a Geant4 modelling for Monte Carlo simulations for the energies released in the LS cocktail. In the present study, Monte Carlo simulations were carried out using a simplified version (*i.e.* without considering the transport of optical photons) of a previous development (Bobin et al., 2016). For each disintegration of ^{60}Co, the results of Monte Carlo simulations are recorded in an output file containing: (i) the position of the disintegration

in the LS volume, (ii) the energies released by the beta decay using β-spectra calculated with the BetaShape code (Mougeot, 2015) and (iii) the energies deposited in the LS volume by the two main γ-photons emitted in cascade (1173 keV and 1332 keV). Because light emision is nonlinear with the deposited energy, the Birks formula (Birks, 1952) was applied to each simulated energy to take into account the attenuation due to ionizing quenching for *kB* values ranging from 80 μm/MeV to 120 μm/MeV. This procedure was implemented to construct two different files (corresponding to 10^6 disintegrations) each representing a different calculation of the predominant allowed β-spectrum with the BetaShape code (with/without exchange effect as displayed in Fig. 1). The two files contain the sum of attenuated energies for each simulated disintegration and for each *kB* parameter mentioned above. The values recorded in these files were used to apply the formalism of the stochastic approach given by Kossert and Grau Carles (2010) to determine the detection efficiency of double coincidences based a minimization procedure (Broda et al., 2007). The asymmetry between PMTs is considered with the use of three individual free parameters related to each PMT. The variability of the stochastic approach was assessed and optimized by means of the bootstrap technique. For each *kB* value ranging from 80 μm/MeV to 120 μm/MeV, the detection efficiency was calculated from $2 \cdot 10^5$ samples randomly drawn with replacement in the total 10^6 simulated disintegrations. This computation was repeated 10 times and the activity concentration for each measurement was assessed using the mean of the results.

The activity concentration determined from the six LS sources filled with UG cocktail was equal to 100.57 (24) kBq/g at the reference date when using the allowed β-spectrum including the atomic effects. The associated uncertainty budget is given in Table 2. The main uncertainty component is related to the TDCR modelling representing the influence of the calculation of the β-spectrum and the variability of the *kB* values The activity concentration is slightly lower (100.38 (24) kBq/g) when the atomic effects are not considered. The same

calculation procedure was implemented in the case of the six LS sources filled with HF cocktail. As displayed in Table 3, the results are in good agreement with those obtained with UG sources. All the results obtained by means of TDCR measurements are displayed in Table 3 for comparison with the result obtained with the 4π(PC)β–γ coincidence method. TDCR analysis for UG sources are also given without considering the γ-emission in the calculation of the detection efficiency. In this case, the detection efficiency is underestimated yielding an activity concentration equal to 100.69 (24) kBq/g when using the allowed β-spectrum including the atomic effects. This result indicates the importance of considering γ-emission in the TDCR analysis to improve the accuracy of activity calculation. As shown in Table 3, the comparison between TDCR and 4π(PC)β–γ anticoincidence measurements shows a better agreement when the calculation of the allowed β-spectrum of ^{60}Co includes the atomic effects. This result is consistent with the findings published in Kossert et al. (2018) for the same radionuclide.

5. Activity measurements of ^{106}Ru/^{106}Rh

5.1 Source preparation

The radioactive solution was purchased from Eckert&Ziegler in the chemical form of Ruthenium chloride in 6 N HCl solution. After dilution, the stock solution of ^{106}Ru/^{106}Rh has a carrier concentration of Ru equal to 124 μg/g and Rh equal to 15 μg/g in 1.4 N HCl solution. The activity concentration was approximately 110 kBq/g at the reference date. The stock solution was also measured by γ-ray spectrometry and no γ-emitting radioactive impurities were found. For TDCR and 4π(LS)β–γ anticoincidence measurements, six LS sources were prepared in standard (low potassium) 20 mL glass vial filled with 10 mL of UG cocktail plus weighed aliquots of the stock solution (masses ranging from 38 mg to 59 mg). The glass vials were coated with diffusive tape prior to measurement. The addition of diffusive tape yields slightly higher experimental TDCR values (~ 0.884) and a downward shift of about 0.2% of the

relationship of double coincidence counting efficiencies versus TDCR. This behavior is due to the low β-energy emission of ^{106}Ru. A similar result was observed for activity measurements of ^{63}Ni and it was investigated using a specific Geant4 model including the transport of optical photons (Thiam et al., 2012). The finding of this study was that the addition of diffusing tape improves the adequation between coincidence measurements and the classical TDCR model by reducing stochastic dependence between PMTs (Bobin et al., 2012). It is noteworthy that the stochastic independence between PMTs is an important condition to avoid a distortion of the Poisson distribution of the mean number of photoelectrons emitted in each PMT for a proper application of the classical TDCR model.

5.2 4π(LS)β–γ anticoincidence measurements

Activity measurements of ^{106}Ru/^{106}Rh with the 4π(LS)β–γ anticoincidence system were performed using a detection system in the β-channel based on a LS counter equipped with XP2020Q PMTs. The 4πβ–γ method was applied in a similar way to the standardization of ^{68}Ge/^{68}Ga (de Silva, 2017; Bobin et al., 2018). The high voltages of the PMTs in the LS channel were decreased to avoid the detection of ^{106}Ru decay events (E_{max} ~ 39.4 keV). The efficacy of the detection threshold was checked by changing the high-voltage values and by adding grey filters. For each 4πβ–γ measurement, coincidence counting was performed using a γ-window centered on the 512-keV energy, which is the most intensive γ-photon emission from ^{106}Rh decay. The efficiency-extrapolation technique was implemented by PMT defocusing and by adding grey filters yielding experimental $\frac{N_c}{N_\gamma}$ values ranging between 0.9 and 0.95 (see Fig. 2). The extrapolation slope estimated from the fitting procedure was equal to 0.26 (2) representing the most significant component in the uncertainty budget given in Table 4. The activity concentration of the ^{106}Ru/^{106}Rh solution was equal to 116.23 (35) kBq/g at the reference date.

5.3 TDCR measurements

In order to achieve the best precision, the comparison between the TDCR and 4π(LS)β–γ methods was carried out with the same LS source used for the application of the efficiency-extrapolation technique. The LS counting was implemented with the same three-PMTs counter used in the β-channel of the 4π(LS)β–γ coincidence system. The maximimum TDCR value was approximately equal to 0.884. The analysis of the TDCR experimental values was carried out using the stochastic approach based on Geant4 simulations already described in the case of ^{60}Co measurements. The β-spectra related to the decay of both ^{106}Ru and ^{106}Rh were considered and calculated using the BetaShape code. The influence of the atomic effects on the β-spectrum calculation was taken into account in the case of ^{106}Ru (see Fig. 3). As for ^{60}Co activity calculations, the TDCR analysis was based on the deposited energies in the LS volume leading to a significant deformation of the energy distribution compared to the calculated β-spectra having energies up to ~3.55 MeV. Indeed, the average of deposited energies shows a reduction of about 25% compared to emitted energies. Because of the high-energy distribution of emitted β-particles and considering that the main β-transition (78.80 (24)%) decays directly to the ground state of ^{106}Pd, the γ-emission was not considered in the TDCR calculations. The ionization quenching function was calculated for each deposited energy using *kB* value ranging from 90 μm/MeV to 120 μm/MeV. The bootstrap technique was applied on 10^6 simulated disintegrations for both ^{106}Ru and ^{106}Rh. The detection efficiency was calculated from $2 \cdot 10^5$ samples randomly drawn with replacement in the total simulated disintegrations and the computation was repeated 10 times.

The activity of the LS source (used for the application of the efficiency-extrapolation technique) was assessed from the mean of seven measurements obtained by PMT defocusing yielding TDCR ranging between 0.874 and 0.884 (see Fig. 4). The result was equal to 4515 (18) Bq at

the reference date when the atomic effects are taken into account. Without the atomic effects, the activity was equal to 4494 (18) Bq. Because the comparison is carried on the same source, the attached uncertainty of both results is mainly related to the TDCR modelling. The value was equal to 0.4% representing the influence of the calculation of the ^{106}Ru β-spectrum, the variability of the *kB* parameters and the variation due to the addition of diffusive tape on glass vial. The activity value given by 4π(LS)β–γ measurements was equal to 4519 (12) Bq. As for the ^{60}Co comparison, a better agreement between the TDCR and 4π(LS)β–γ methods is obtained when the atomic effects are taken into account (see Table 5). The deviation with 4π(LS)β–γ anticoincidence counting is larger (~ 0.5%) when the atomic effects are not considered.

The activity concentration of the stock solution of ^{106}Ru/^{106}Rh was assessed from the results obtained with all the LS samples in the same manner as described above. The mean value was equal to 116.13 (51) kBq/g at the reference date when using the allowed β-spectrum of ^{106}Ru including the atomic effects. The uncertainty budget is given in Table 6. A good agreement with the result given by 4π(LS)β–γ anticoincidence was obtained.

6. Discussion

The present investigations provide a new confirmation that a better agreement between the TDCR and 4πβ–γ coincidence methods is obtained when the atomic screening and exchange effects are taken into account in β-spectra calculations. The same findings published by Kossert et al. (2018) were obtained in the case of the activity standardization of ^{60}Co. Regarding the ^{106}Ru/^{106}Rh activity measurements, the deviation between the TDCR and 4πβ–γ coincidence methods is larger when the atomic effects are not considered (~ 0.5%). Based on the present study, the same recommendation as given for TDCR measurements of ^{55}Fe (Ziemek et al., 2022) can be made on the use of LS vials with diffusing walls for the activity standardization of

^{106}Ru/^{106}Rh. An uncertainty component related to the TDCR modelling of about 0.4% should be assigned to take into account the sensitivity of ^{106}Ru β-spectrum calculation. The analysis of the experimental TDCR measurements was based on a new stochastic model based on Geant4 simulations. Further developments and improvements are in progress by including the PenNuc package (García-Toraño et al., 2019) for a more detailed description of nuclear decay pathways, in particular for the standardization of electron-capture radionuclides (e.g. ^{55}Fe, ^{51}Cr, ^{85}Sr, ^{125}I).

References

Agostinelli, S., et al., 2003. Geant4 – a simulation toolkit. Nucl. Instrum. Methods A 506, 250-303.

Angrave, L.C., Booth, N.E., Gaitskell, R.J., Salmon, G.L., 1998. Measurement of the Atomic Exchange Effect in Nuclear β Decay. Physical Review Letters 80, Number 8, 1610-1613.

Aprile, E., et al. (XENON Collaboration), 2020. Excess electronic recoil events in XENON1T. Phys. Rev. D 102, 072004.

Baerg, A.P., 1973. The efficiency extrapolation method in coincidence counting. Nucl. Instrum. Methods 112, 143-150.

Baerg, A.P., Munzenmayer, K., Bowes, G. C. 1976. Live-Timed Anti-Coincidence Counting with Extending Dead-Time Circuitry. Metrologia 12, 77-80.

Bé, M.-M., Chisté, V., Dulieu, C., Browne, E., Baglin, C., Chechev, V.P., Kuzmenko, N.K., Helmer, R., Kondev, F., MacMahon, D., Lee, K.B., 2006. Monographie BIPM-5, Table of Radionuclides, vol. 3. Bureau International des Poids et Mesures. ISBN 92-822-2218-7.

Bé, M.-M., Chisté, V., Dulieu, C., Kellett, M.A., Mougeot, X., Arin, A., Chechev, V.P., Kuzmenko, N.K., Kibédi, T., Luca, A., Nichols, A.L., 2016. Monographie BIPM-5, Table of Radionuclides, vol. 8. Bureau International des Poids et Mesures. ISBN 92-822-2264-5.

Birks, J.B., 1952. Theory of the response of organic scintillation crystals to short-range particles. Phys. Rev. 86, 56

Bobin, C., 2007. Primary standardization of activity using the coincidence method based on analogue instrumentation. Metrologia 44, S27-S31.

Bobin, C., Thiam, C., Chauvenet, B., Bouchard, J., 2012. On the stochastic dependence between photomultipliers in the TDCR method. Appl. Radiat. Isot. 70, 770-780.

Bobin, C., Thiam, C., Bouchard, J., 2016. Calculation of extrapolation curves in the 4π(LS)β-γ coincidence technique with the Monte Carlo code Geant4. Appl. Radiat. Isot. 109, 319-324.

Bobin, C., Thiam, C., Bouchard, J., 2018. Standardization of ^{68}Ge/^{68}Ga using the 4πβ–γ coincidence method based on Cherenkov counting. Appl. Radiat. Isot. 134, 252-256.

Bouchard, J., 2000. MTR2: a discriminator and dead-time module used in counting systems. Appl. Radiat. Isot. 52, 441-446.

Bouchard, J., Cassette, P., 2000. MAC3: an electronic module for the processing of pulses delivered by a three photomultiplier liquid scintillation counting system. Appl. Radiat. Isot. 52, 669-672.

Bouchard., J., 2022. A new set of electronic modules (NIM standard) for a coincidence system using the pulse mixing method. Appl. Radiat. Isot. 56, 269-273.

Broda, R., Cassette, P., Kossert, K., 2007. Radionuclide metrology using liquid scintillation counting. Metrologia 44, S36–S52.

Bühring, W., 1984. The screening correction to the fermi function of nuclear β-decay and its model dependence. Nucl. Phys. A 430, 1-20.

Campion, P. J., 1959. The standardization of radioisotopes by the beta-gamma coincidence method using high efficiency detectors. Int. J. Appl. Radiat. Isot. 101, 232-248.

Gaitskell, R.J., Angrave, L.C., Booth, N.E., Hahn, A.D., Salmon, G.L., Swift, A.M., 1996. A measurementof the beta spectrum of ^{63}Ni using a new type of calorimetric cryogenic detector. Nucl. Instrum. Methods A 370, 250-252.

García-Toraño, E., Peyres, V., Salvat, F., 2019. PenNuc: Monte Carlo simulation of the decay of radionuclides. Computer Physics Communications 245, 106849.

Kossert, K., Grau Carles, A., 2010. Improved method for the calculation of the counting efficiency of electron-capture nuclides in liquid scintillation samples. Appl. Radiat. Isot. 68, 1482-1488.

Kossert, K., Mougeot, X., 2015. The importance of the beta spectrum calculation for accurate activity determination of ^{63}Ni by means of liquid scintillation counting. Appl. Radiat. Isot. 101, 40-43.

Kossert, K., Marganiec-Gałązka, J., Mougeot, X., Nähle, O. J., 2018. Activity determination of ^{60}Co and the importance of its beta spectrum. Appl. Radiat. Isot. 134, 212-218.

Kossert, K., Mougeot, X., 2021. Improved activity standardization of ^{90}Sr/^{90}Y by means of liquid scintillation counting. Appl. Radiat. Isot. 168, 109478.

Loidl, M., Le-Bret, C., Rodrigues, M., Mougeot, X., 2014. Evidence for the exchange effect down to very low energy in the beta decays of ^{63}Ni and ^{241}Pu. Journal of Low Temp. Phys. 176, 1040-1045.

Mougeot, X., Bé, M.-M., Bisch, C., Loidl, M., 2012. Evidence for the exchange effect in the beta decay of ^{241}Pu. Phys. Rev. A 86, 042506.

Mougeot, X., Bisch C., 2014. Consistent calculation of the screening and exchange effects in allowed β- transitions. Phys. Rev. A 90, 012501 (2014).

Mougeot, X., 2015. Erratum: Reliability of usual assumptions in the calculation of β and ν spectra. Phys. Rev. C 92, 059902.

Pyper, N.C., Harston, M.R., 1988. Atomic effects on β-decay. Proc. R. Soc. Lond. A 420, 277-321.

Sibbens, G., Altzitzoglou, T., 2007. Preparation of radioactive sources for radionuclide metrology. Metrologia 44, S71-S78.

da Silva, C.J., Rezende, E.A., Poledna, R., Tauhata, L., Iwahara, A., Lopes, R.T., 2017. Standardization of ^{106}Ru/Rh by live-timed anticoincidence counting and gamma emission determination. Appl. Radiat. Isot. 122, 37-40.

Thiam, C., Bobin, C., Chauvenet, B., Bouchard, J., 2012. Application of TDCR-Geant4 modeling to standardization of ^{63}Ni. Appl. Radiat. Isot. 70, 2195-2199.

Turkat, S., Mougeot, X., Singh, B., Zuber, K., 2023. Systematics of logft values for β−, and EC/β+ transitions. Atomic Data and Nuclear Data Tables 152, 101584.

Ziemek, T., Broda, R., Listkowska, A., Lech, E., Dziel, T., Saganowki, P., Tyminski, Z., 2022. Standardization of an ^{55}Fe solution using the TDCR method in POLATOM as part of the CCRI(II)-K2.Fe-55.2019 key comparison. Journal of Radioanalytical and Nuclear Chemistry 331, 3241-3248.

Captions

Table 1: Uncertainty budget related to the activity concentration of ^{60}Co obtained by 4π(PC)β–γ anticoincidence counting.

Table 2: Uncertainty budget related to the activity concentration of ^{60}Co obtained by TDCR counting in the case of LS sources prepared with UG cocktail.

Table 3: Comparison of the activity concentration results of ^{60}Co (in kBq/g) obtained by TDCR and 4π(PC)β–γ anticoincidence counting. TDCR values are given using β-spectra calculated with and without atomic effects.

Table 4: Uncertainty budget related to the activity concentration of ^{106}Ru/^{106}Rh obtained by 4π(LS)β–γ anticoincidence counting.

Table 5: Comparison of the activity results of ^{106}Ru/^{106}Rh obtained by TDCR and 4π(LS)β–γ anticoincidence counting for the same LS sample used for the application of the efficiency-extrapolation technique. The TDCR values are given using β-spectra of ^{106}Ru calculated with and without atomic effects.

Table 6: Uncertainty budget related to the activity concentration of ^{106}Ru/^{106}Rh obtained by TDCR counting.

Figure 1: Comparison of the theoretical β-energy spectra for the allowed main transition of ^{60}Co computed using the BetaShape code with and without considering the atomic effects.

Figure 2: Efficiency-extrapolation curve in the case of 4π(LS)$\beta-\gamma$ anticoincidence counting of ^{106}Rh. A detection threshold is applied to avoid ^{106}Ru counting in the β-channel. The uncertainty bars in both axis correspond to counting statistics.

Figure 3: Comparison of the theoretical β-energy spectra for the allowed transition of ^{106}Ru computed using the BetaShape code with and without considering the atomic effects.

Figure 4: Activity results for TDCR measurements of ^{106}Ru/^{106}Rh obtained by PMT defocusing for the same LS sample used for the application of the efficiency-extrapolation technique. The uncertainty bars correspond to counting statistics

Table 1

Uncertainty component	Comment	*u(a)/a* (%)
Statistics	Standard deviations on source measurements	0.06
Background		0.02
Weighing	Gravimetric measurements using the pycnometer method	0.1
Live time technique	MTR2 modules in both β- and γ-channels	0.02
Decay correction		negligible
Efficiency extrapolation		0.08
Relative combined standard uncertainty		0.14

Table 2

Uncertainty component	Comment	*u(a)/a* (%)
Statistics	Standard deviations on source measurements	0.09
Background		0.03
Weighing	Gravimetric measurements using the pycnometer method	0.1
Live time technique	MAC3 module	0.02
Decay correction		negligible
TDCR Model	Stochastic approach based on Geant4 simulations	0.2
Relative combined standard uncertainty		0.24

Table 3

4π(PC)β–γ anticoincidence	TDCR / UG sources			TDCR / HF sources	
100.58 (14)	With atomic effect	With atomic effect Without γ-emission	Without atomic effect	With atomic effect	Without atomic effect
	100.57 (24)	100.69 (24)	100.38 (24)	100.65 (24)	100.40 (24)

Table 4

Uncertainty component	Comment	*u(a)/a* (%)
Statistics	Standard deviations on source measurements	0.06
Background		0.1
Weighing	Gravimetric measurements using the pycnometer method	0.1
Live time technique	MTR2 modules in both β- and γ-channels	0.02
Decay correction		0.1
Efficiency extrapolation technique		0.24
Relative combined standard uncertainty		0.3

Table 5

4π(LS)β–γ anticoincidence	TDCR / UG sources	
4519 (12) Bq	With atomic effect	Without atomic effect
	4515 (18) Bq	4494 (18) Bq

Table 6

Uncertainty component	Comment	*u(a)/a* (%)
Statistics	Standard deviations on source measurements	0.11
Background		0.02
Weighing	Gravimetric measurements using the pycnometer method	0.1
Live time technique	MAC3 module	0.02
Decay correction		0.1
TDCR Model	Stochastic approach based on Geant4 simulations	0.4
Relative combined standard uncertainty		0.44

Figure 1

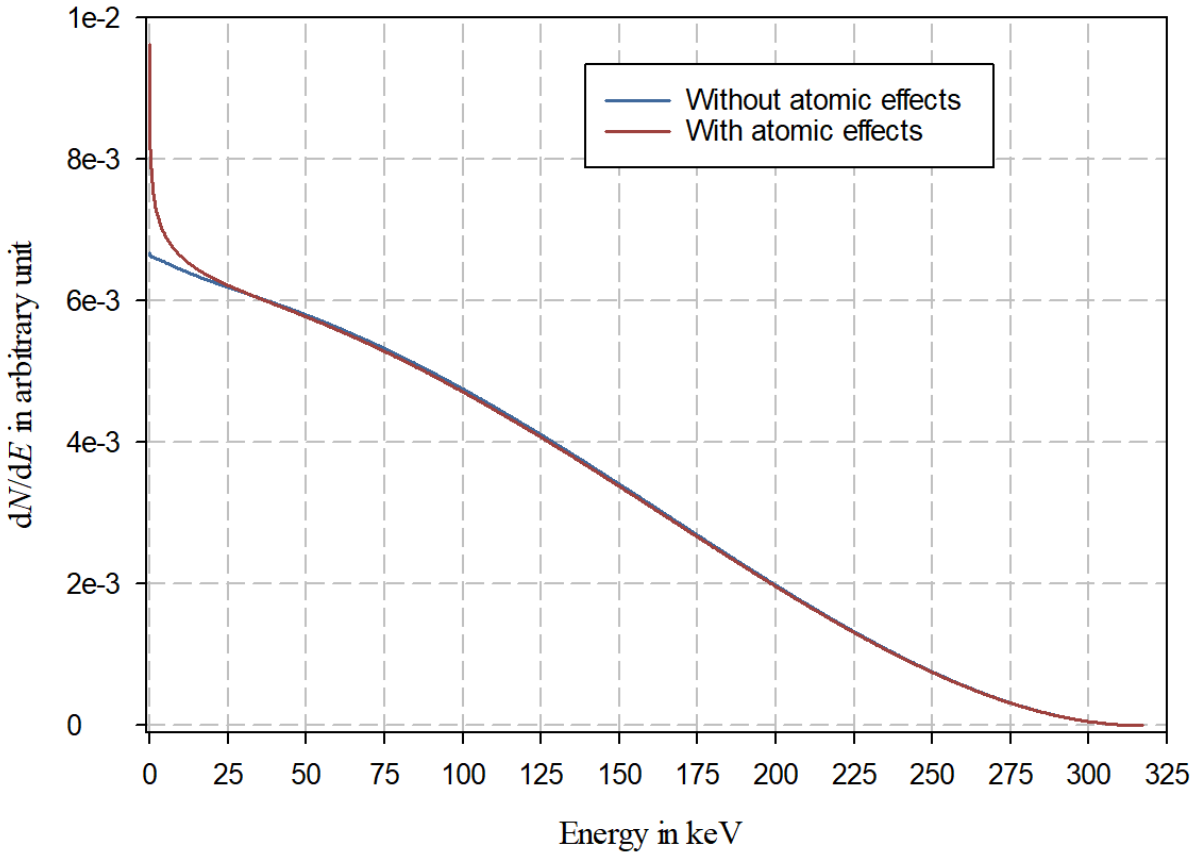
1e-2
8e-3
6e-3
4e-3
2e-3
0
dN/dE in arbitrary unit
0
25
50
75
100
125
150
175
200
225
250
275
300
325
Energy in keV
Without atomic effects
With atomic effects

Figure 2

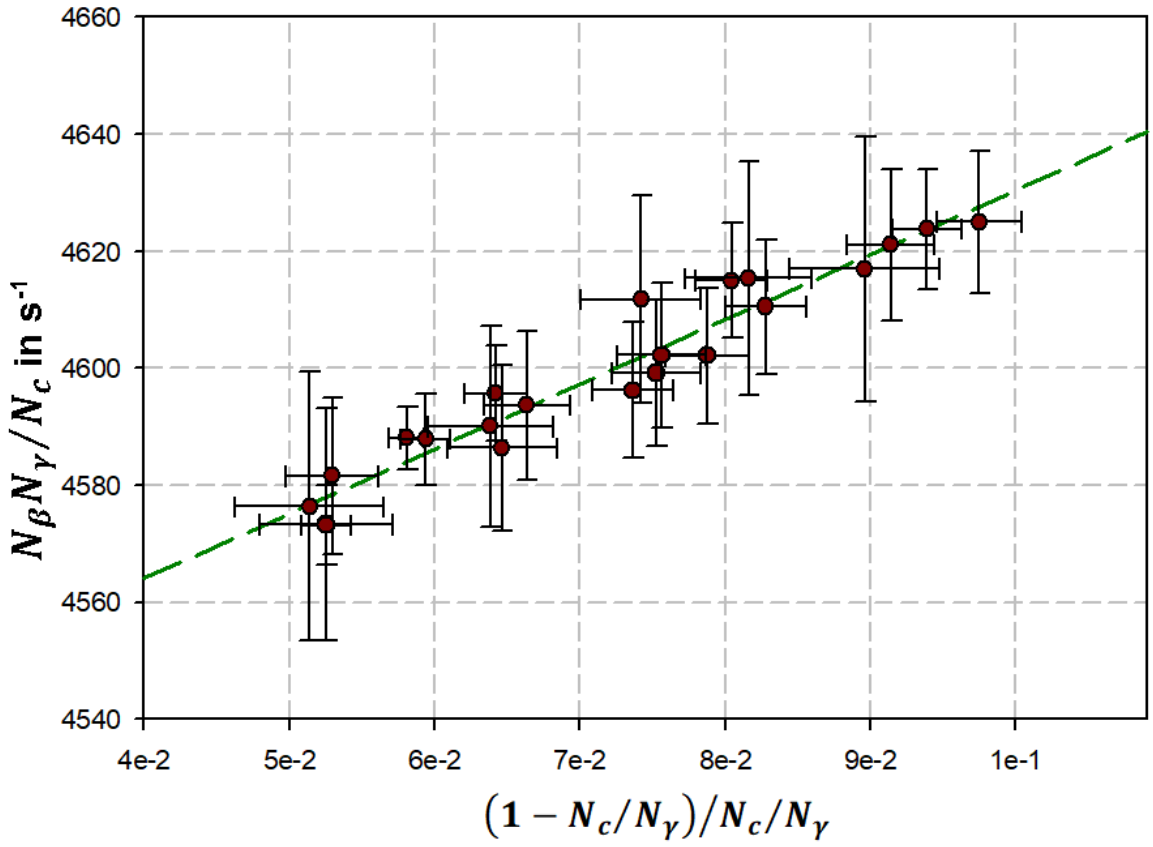
4660
4640
4620
4600
4580
4560
4540
$N_\beta N_\gamma / N_c$ in s^{-1}
4e-2
5e-2
6e-2
7e-2
8e-2
9e-2
1e-1
$(1 - N_c/N_\gamma)/N_c/N_\gamma$

Figure 3

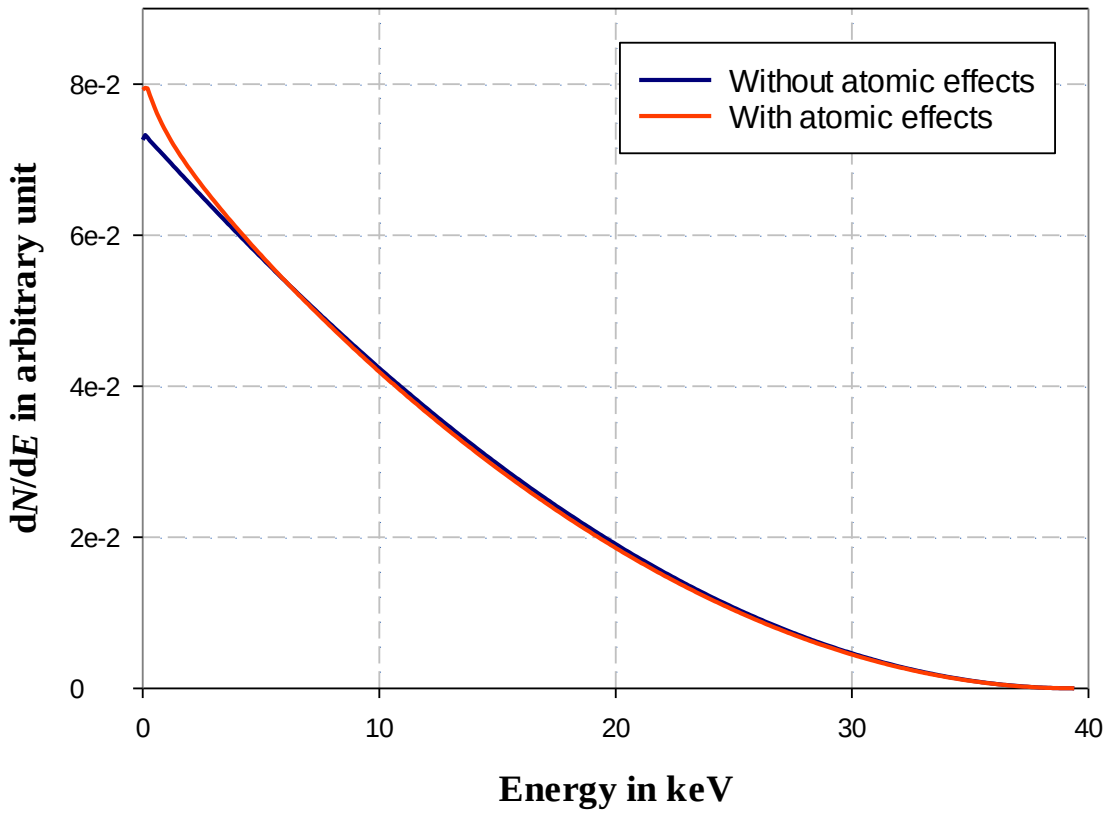
Without atomic effects
With atomic effects
8e-2
6e-2
4e-2
2e-2
0
0
10
20
30
40
dN/dE in arbitrary unit
Energy in keV

Figure 4

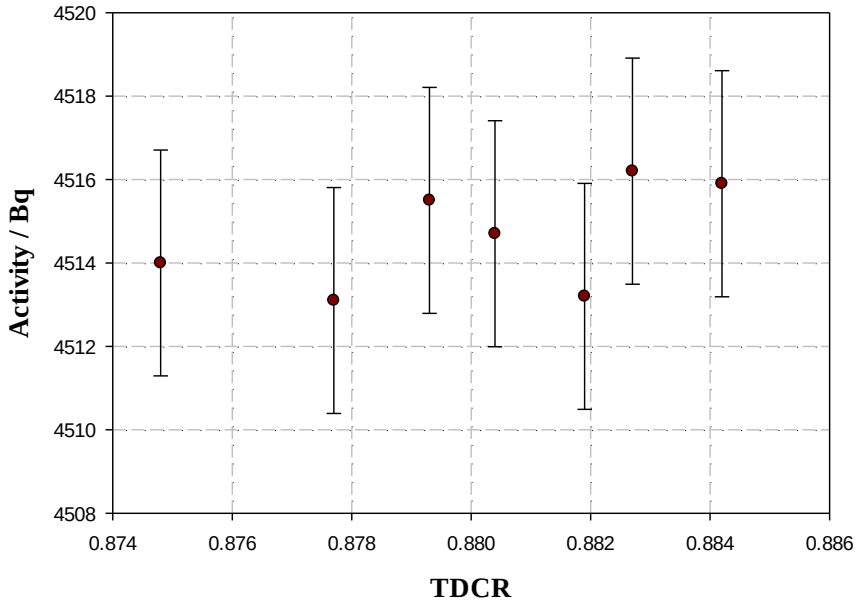
4520
4518
4516
4514
4512
4510
4508
Activity / Bq
0.874
0.876
0.878
0.880
0.882
0.884
0.886
TDCR